Influences of impregnation ratio and activation time on ultramicropores of peanut shell active carbons

ARTICLE *in* MATERIALS LETTERS · FEBRUARY 2015

Impact Factor: 2.27 · DOI: 10.1016/j.matlet.2014.11.042

5 AUTHORS, INCLUDING:

Lingzhao Kong
Chinese Academy of Sciences
19 PUBLICATIONS **161** CITATIONS

SEE PROFILE

Materials Letters 141 (2015) 340–343

Contents lists available at ScienceDirect

Materials Letters

journal homepage: www.elsevier.com/locate/matlet

Influences of impregnation ratio and activation time on ultramicropores of peanut shell active carbons

Dawei Li [a,d,e], Conglai Li [b], Yuanyu Tian [a,*], Lingzhao Kong [c,**], Li Liu [d]

[a] State Key Laboratory of Heavy Oil Processing, China University of Petroleum (East China), Qingdao 266555, China
[b] Qingdao Hisense Hitachi Air-conditioning Systems Co., Ltd., Qingdao 266510, China
[c] Shanghai Advanced Research Institute, Chinese Academy of Sciences, Shanghai 201210, China
[d] Key Laboratory of Chemical Utilization of Forestry Biomass of Zhejiang Province, Zhejiang A & F University, Lin'an 311300, China
[e] Key Laboratory of Wood Science and Technology, Lin'an 311300, China

ARTICLE INFO

Article history:
Received 1 September 2014
Accepted 12 November 2014
Available online 24 November 2014

Keywords:
Carbon material
Porous material
Peanut shell
Ultramicropore
Activation time
Impregnation ratio

ABSTRACT

We studied effects of impregnation ratio and activation time on ultramicropores of KOH-activated peanut shell active carbons (ACs). The ultramicropores were characterized in terms of ultramicropore volume ($V_{<0.7\ nm}$), ultramicropore fraction ($V_{<0.7\ nm}/V_t$), and pore size distribution. The ultramicropores of the ACs were mostly in the range of 0.45–0.70 nm. Increasing the impregnation ratio from 1 to 3 first increased the $V_{<0.7\ nm}$ and $V_{<0.7\ nm}/V_t$, and then decreased them. Prolonging the activation time from 1 h to 2 h resulted in a minimum $V_{<0.7\ nm}/V_t$, but hardly affected the $V_{<0.7\ nm}$. The AC with the highest $V_{<0.7\ nm}$ (0.11 ml/g) was obtained by activation for 1–2 h at an impregnation ratio of 2. The $V_{<0.7\ nm}$ bore a linear relationship with the CO_2 uptakes at 0.1 and 0.2 bar (0 °C). This research was significant for preparation of ACs with developed ultramicropores.

1. Introduction

Preparation of active carbons (ACs) from peanut shells has aroused much interest [1–5], due to the abundant availability of the shells and wide applications of the ACs [6–9]. So far, peanut shell ACs have been prepared by activation using various agents including KOH [2–5,7,8], with much attention paid to effects of process parameters on pore properties like surface area and pore volume. However, the influences of process parameters on ultramicropores of peanut shell ACs remain unknown.

According to IUPAC classification, ultramicropores are the pores with sizes less than 0.7 nm [10]. Such pores have been found highly important for adsorption of some gases like CO_2 [10,11] and H_2 [12–14]. Hence, knowing how ultramicropores vary with process parameters is necessary for improving gas separation or storage.

This research aimed to investigate effects of impregnation ratio and activation time on ultramicropores of KOH-activated peanut shell ACs. The ACs were characterized in terms of surface morphology and pore properties such as ultramicropore size distribution, ultramicropore volume, and ultramicropore fraction. The research could provide guidelines for preparation of highly ultramicroporous ACs.

2. Experimental

Active carbons (ACs) were prepared by KOH activation of peanut shell char (PSC), with the KOH and PSC described in Text S1 of Supplementary material (SM). To prepare ACs, 4.00 g of PSC with sizes of 0.28–0.90 mm was mixed with KOH dissolved in 14-ml distilled water at an impregnation ratio (KOH/PSC weight ratio) of 1–3. After being shaken for 5 h, the mixture was dehydrated at 140 °C under N_2 until constant weight. Subsequently, the dried mixture was heated in N_2 flow first to 400 °C with a retention time of 30 min at a heating rate of 8 °C/min, and then to 780 °C with a retention time of 1–2 h at 10 °C/min. The as-obtained sample was cooled, washed repeatedly with distilled water until the washings were about neutral, and finally dried at 110 °C overnight. The prepared active carbon was named AC*x*–*y* h, where *y* h and *x* denoted activation time in hours and impregnation ratio, respectively. For example, AC1–2 h represented an active carbon prepared by activation for 2 h at an impregnation ratio of 1 using the aforementioned process.

Surface morphology of samples was observed using a scanning electron microscope (SEM, S4800, Hitachi Corp., Japan). N_2 adsorption/desorption isotherms at 77 K were measured by a static

* Corresponding author. Tel.: +86 532 86057035.
** Corresponding author. Tel.: +86 21 20350944.
E-mail addresses: shuxuewuli@126.com (Y. Tian), konglz@sari.ac.cn (L. Kong).

http://dx.doi.org/10.1016/j.matlet.2014.11.042
0167-577X/

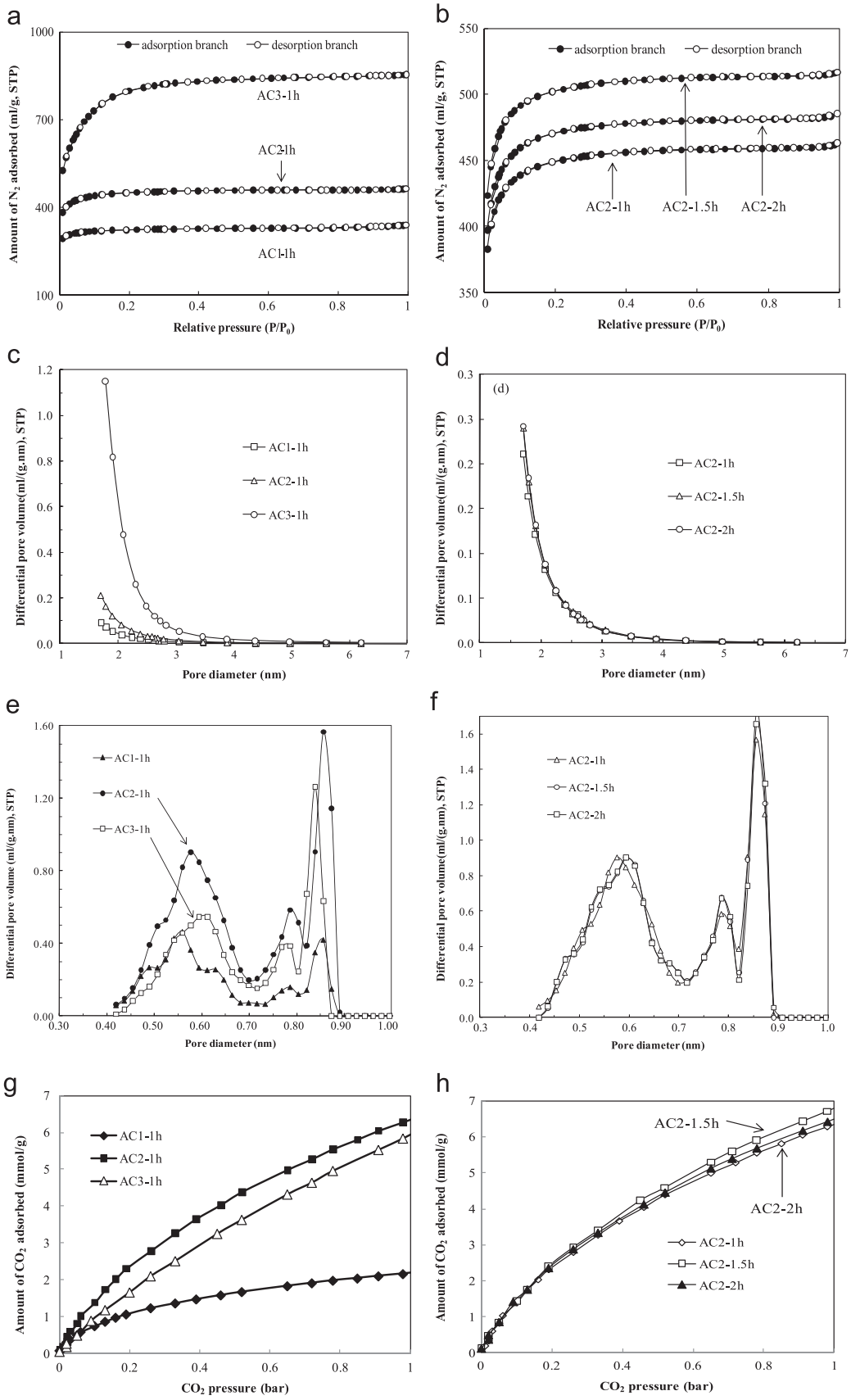

Fig. 1. N_2 adsorption/desorption isotherms (a, b), mesopore size distributions (c, d), ultramicropore size distributions (e, f), and CO_2 adsorption isotherms at 0 °C (g, h) of active carbons activated for 1–2 h at impregnation ratios of 1–3.

Table 1
Pore properties and CO_2 uptakes (0 °C) of active carbons.

Samples	S_{BET} (m^2/g)	V_t (ml/g)	V_{micro} (ml/g)	V_{meso} (ml/g)	$V_{<0.7\ nm}$ (ml/g)	V_{lm}[a] (ml/g)	V_{micro}/V_t (%)	$V_{<0.7\ nm}/V_t$ (%)	CO_2 uptakes at 0.1/0.2 bar (mmol/g)
Effect of impregnation ratio									
AC1–1 h	1195	0.52	0.50	0.02	0.05	0.45	96.1	10.1	0.75/1.07
AC2–1 h	1670	0.71	0.71	0.01	0.11	0.60	98.8	14.8	1.42/2.34
AC3–1 h	3013	1.32	1.28	0.04	0.06	1.22	97.1	4.8	0.94/1.69
Effect of activation time									
AC2–1 h	1670	0.71	0.71	0.01	0.11	0.60	98.8	14.8	1.42/2.34
AC2–1.5 h	1871	0.82	0.80	0.02	0.11	0.69	97.8	12.9	1.48/2.43
AC2–2 h	1752	0.75	0.74	0.01	0.11	0.63	98.7	14.2	1.46/2.40

[a] V_{lm}: volume of large micropores (0.7–2 nm) calculated by subtracting $V_{<0.7\ nm}$ from V_{micro}.

volumetric analyzer (TristarII3020, Micromeritics, USA). The adsorption isotherms were used to calculate specific surface area (S_{BET}), total pore volume (V_t), micropore volume (V_{micro}), mesopore size distribution, mesopore volume (V_{meso}), and micropore fraction (V_{micro}/V_t), with the calculation methods presented in Text S1 of Supplementary material (SM). CO_2 adsorption at 0 °C was performed using another static volumetric analyzer (ASAP2020, Micromeritics, USA). Based on the adsorption isotherms, the volume ($V_{<0.7\ nm}$) and pore size distribution of ultramicropores were obtained using the non-local density functional theory and a slit-pore model. Before adsorption of gases, ACs were degassed under vacuum at 250 °C for at least 3 h. XRD patterns were obtained on an X-ray diffractometer (Max2500PC, MacScience Corp., Japan) at an acceleration voltage of 30 kV.

3. Results and discussion

Fig. S1 in the Supplementary material (SM) shows that the active carbon (AC2–1.5 h) displayed rougher surfaces and more pores than the PSC and peanut shell, which reflected the activation effects of KOH. The XRD patterns of ACs exhibited broad peaks around 23° and 42° (Fig. S2, SM), indicating that the carbon structure of the ACs was amorphous. The N_2 adsorption/desorption isotherms (Fig. 1a and b) of all ACs were type I (IUPAC classification), indicating that the ACs were microporous. This result was also reflected by their high microporosity (V_{micro}/V_t, Table 1) and low mesopore-size-distribution curves (Fig. 1c and d). The S_{BET} and V_t of the ACs changed markedly as the impregnation ratio and activation time changed (Table 1), due to the variation of V_{micro}. The variation of V_{micro} was due to the redox reaction of KOH with carbon to form carbonate, followed by activation with CO_2 from carbonate decomposition and K metal intercalation between graphene layers [15,16].

The ultramicropore sizes of the ACs activated at different impregnation ratios were mostly in the range of 0.45–0.70 nm (Fig. 1e). The impregnation ratio was found to markedly affect the ultramicropores. As the impregnation ratio increased from 1 to 2, more KOH reacted with the char, causing removal of more elements like carbon from the char and creation of ultramicropores; thus, compared with AC1–1 h, AC2–1 h exhibited a lower yield (Table S1, SM), but a larger $V_{<0.7\ nm}$ (Table 1) and a higher ultramicropore size distribution curve (UPSDC) (Fig. 1e). When the impregnation ratio increased from 2 to 3, the further removal of elements, as shown by the low yield of AC3–1 h (Table S1, SM), caused enlargement of ultramicropores into large micropores; thus, compared with AC2–1 h, AC3–1 h showed a higher V_{lm} but a lower $V_{<0.7\ nm}$ and UPSDC.

When the impregnation ratio varied, the fraction of ultramicropores ($V_{<0.7\ nm}/V_t$) peaked at an impregnation ratio of 2 (Table 1). This trend was because the fraction was dominated by $V_{<0.7\ nm}$. Hence, AC2–1 h having the largest $V_{<0.7\ nm}$ showed the highest $V_{<0.7\ nm}/V_t$ (Table 1).

The ultramicropore sizes were mostly in the range of 0.45–0.70 nm for the ACs prepared at different activation times (Fig. 1f). The UPSDCs of these ACs almost overlapped, indicating that the ACs had similar ultramicropore size distributions. This similarity was also supported by the fact that these samples had nearly the same $V_{<0.7\ nm}$ (Table 1). Thus, the activation time hardly affected the ultramicropore size distribution and $V_{<0.7\ nm}$. This result was ascribable to the fact that increasing the activation time failed to further remove elements from the char, as reflected by the observation that the yields were similar for the samples activated for different times (Table S1, SM); hence, few ultramicropores were formed.

However, the increment in activation time from 1 h to 2 h varied the ultramicropore fraction ($V_{<0.7\ nm}/V_t$, Table 1), because V_t was changed. The V_t increased with increasing the activation time from 1 h to 1.5 h, due to the rise in V_{micro} caused by creation of large micropores (0.7–2 nm) as reflected by the increased V_{lm}, whereas the V_t decreased with further increasing the activation time to 2 h, mainly ascribable to the reduced V_{lm} caused by carbon skeleton contraction (Table 1). Thus, $V_{<0.7\ nm}/V_t$ first decreased and then increased with prolonging the activation time from 1 h to 2 h.

Plots of $V_{<0.7\ nm}$ of the obtained ACs versus their CO_2 uptakes at 0.1 bar and 0.2 bar were both linear, with linear correlation coefficients (R^2) being 0.994 and 0.945, respectively (Fig. S3, SM). These results indicated that adsorption of CO_2 at low pressures was dominated by ultramicropore volume, as found by Hao [17]. Hence, study on the effects of process parameters on ultramicropores was significant for CO_2 separation from gas mixture whose CO_2 partial-pressure was low, such as flue gas from conventional coal-fired power plants (typical partial pressure of CO_2 <0.2 bar) [17]. The importance of ultramicropores for CO_2 adsorption was also reflected by the fact that rice husk ACs showing a higher $V_{<0.7\ nm}$ than the peanut shell ACs (0.15 ml/g > 0.11 ml/g) displayed a higher CO_2 uptake (2.11 mmol/g > 1.48 mmol/g, 0.1 bar, 0 °C) [18].

4. Conclusions

Study was conducted on the effects of impregnation ratio and activation time on ultramicropores of KOH-activated peanut-shell active carbons. The ultramicropores were mostly between 0.45 nm and 0.70 nm. With increasing the impregnation ratio from 1 to 3, the ultramicropore volume ($V_{<0.7\ nm}$) and ultramicropore fraction ($V_{<0.7\ nm}/V_t$) first increased and then decreased. With increasing the activation time from 1 h to 2 h, the $V_{<0.7\ nm}$ hardly varied, but the $V_{<0.7\ nm}/V_t$ first diminished and then rose. The sample with the highest $V_{<0.7\ nm}$ (0.11 ml/g) was obtained by activation for 1–2 h using an impregnation ratio of 2. The $V_{<0.7\ nm}$ bore a significant linear relationship with the CO_2 uptakes at 0.1 bar and 0.2 bar (0 °C).

Acknowledgments

We acknowledge the National Natural Science Foundation of China (51206099), Program for New Century Excellent Talent in University of the Ministry of Education of China (NCET-11-1031), Zhejiang Provincial Key Laboratory of Chemical Utilization of Forestry Biomass, and Zhejiang Key Level 1(2014LYGCZ019).

Appendix A. Supplementary material

Supplementary material associated with this article can be found in the online version at http://dx.doi.org/10.1016/j.matlet.2014.11.042.

References

[1] Lochananon W, Chatsiriwech DJ. Ind Eng Chem 2008;14:84–8.
[2] Girgis BS, Soliman AM, Fathy NA. Microporous Mesoporous Mater 2011;142:518–25.
[3] Guo PZ, Ji QQ, Zhang LL, Zhao SY, Zhao XS. Acta Phys Chim Sin 2011;27:2836–40.
[4] Zhong ZY, Yang Q, Li XM, Luo K, Liu Y, Zeng GM. Ind Crops Prod 2012;37:178–85.
[5] Wu M, Guo QJ, Fu GJ. Powder Technol 2013;247:188–96.
[6] Gonzo EE, Gonzo LF. Adsorpt Sci Technol 2008;26:651–9.
[7] Al-Othman ZA, Ali R, Naushad M. Chem Eng J 2012;184:238–47.
[8] He XJ, Ling PH, Qiu JS, Yu MX, Zhang XY, Yu C, et al. J Power Sources 2013;240:109–13.
[9] Zhang JX, Ou LL. Water Sci Technol 2013;67:737–44.
[10] Jimenez V, Ramirez-Lucas A, Diaz JA, Sanchez P, Romero A. Environ Sci Technol 2012;46:7407–14.
[11] De Souza LKC, Wickramaratne NP, Ello AS, Costa MJF, da Costa CEF, Jaroniec M. Carbon 2013;65:334–40.
[12] Silvestre-Albero AM, Wahby A, Silvestre-Albero J, Rodriguez-Reinoso F, Betz W. Ind Eng Chem Res 2009;48:7125–31.
[13] Vargas DP, Giraldo L, Silvestre-Albero J, Moreno-Pirajan JC. Adsorption 2011;17:497–504.
[14] Cai JJ, Qi JB, Yang CP, Zhao XB. ACS Appl Mat Interfaces 2014;6:3703–11.
[15] Wang JC, Heerwig A, Lohe MR, Oschatz M, Borchardt L, Kaskel SJ. Mater Chem 2012;22:13911–3.
[16] Labus K, Gryglewicz S, Machnikowski J. Fuel 2014;118:9–15.
[17] Hao W, Bjorkman E, Lilliestrale M, Hedin N. Appl Energy 2013;112:526–32.
[18] Li D, Ma T, Zhang R, Tian Y, Qiao Y. Fuel 2015;139:68–70.